AR-NE3A /2014G563

Structural and computational study on inhibitory compounds for endonuclease activity of influenza virus polymerase

Tyuji Hoshino[1,*] Satoshi Fudo[1] and Michiyoshi Nukaga[2]
[1] Graduate School of Pharmaceutical Sciences, Chiba University,
1-8-1 Inohana, Chuo-ku, Chiba 260-8675, Japan
[2] Faculty of Pharmaceutical Sciences, Josai International University,
Gumyo 1, Togane-shi Chiba 283-8555, Japan

1 Introduction

Seasonal epidemics and occasional pandemics caused by influenza viruses are global threats to humans. Since the efficacy of currently approved drugs is limited by the emerging resistance of the viruses, the development of new antiviral drugs is still demanded. Endonuclease activity, which lies in the influenza polymerase acidic protein N-terminal domain (PA_N), is a potent target for novel antiviral agents. Here, we report the identification of some novel inhibitors for PA_N endonuclease activity. The binding mode of one of the inhibitory compounds to PA_N was investigated in detail by means of X-ray crystal structure analysis and molecular dynamics (MD) simulation [1].

2 Experiment

Chemical screening for PA_N endonuclease inhibitors was conducted with compound stock in our research team. Single-stranded DNA plasmid M13mp18 (5 ng/μl) was incubated in the reaction buffer (20 mM Tris-HCl pH 7.5, 100 mM NaCl, 10 mM β-mercaptoethanol, and 1.0 mM $MgCl_2$) in the presence of 1.0 mg/mL PA_N and 100 μM of each compound from our library for 60 min at 37 °C. The reaction was stopped by adding 20 mM EDTA. The reaction products were loaded on a 0.8% agarose gel for electrophoresis and stained with ethidium bromide.

Crystals of $PA_N^{\Delta loop}$ were grown by vapor diffusion in hanging drops containing 1.0 μL of 9.9 mg/mL protein solution including 4.0 mM $MnCl_2$ and 1.0 μL of well solution (100 mM MES [pH 5.8], 1.1 M ammonium sulfate, 0.1 M potassium chloride and 9% (v/v) trehalose) at 18°C. Crystals were soaked with well solution containing 10.0 mM $MnCl_2$ and 4.0 mM compound **1** for 2.0 hours. The crystals were then cryo-protected by brief immersion in well solution containing 22.5% (v/v) glycerol followed by flash-freezing in liquid nitrogen.

X-ray diffraction data were collected at 100 K with a wavelength of 1.0 Å on the AR-NE3A beamline of photonfactory (PF, Tsukuba, Japan). The diffraction data were indexed, scaled and merged with HKL2000. Intensities were converted into structure factors and 5% of the reflections were flagged for R_{free} calculations. The $PA_N^{\Delta loop}$ structure was determined by molecular replacement using the program MOLREP with the crystal structure 4M5Q (PDB code) as a search model. Structure refinement and model building were carried out using PHENIX and COOT.

3 Results and Discussion

We first carried out an in vitro chemical screening for finding endonuclease inhibitors with approximately 410 compounds. The screening resulted in the identification of several PA_N endonuclease inhibitors including compounds **1**, **2**, and **3** (Fig 1).

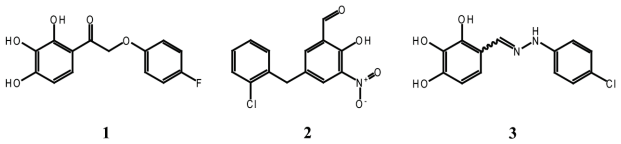

1 **2** **3**

Figure 1: Structures of compounds identified as inhibitors of PA_N endonuclease activity.

Compounds bearing a trihydroxyphenyl group have already been suggested to show inhibitory activity against PA_N. Compounds **1** and **3** contain a trihydroxyphenyl moiety, but they have not been reported as inhibitors for PA_N. Compound **2** has a different scaffold. We carried out a FRET-based endonuclease assay for measurement of the IC_{50} values of these compounds (Fig. 2).

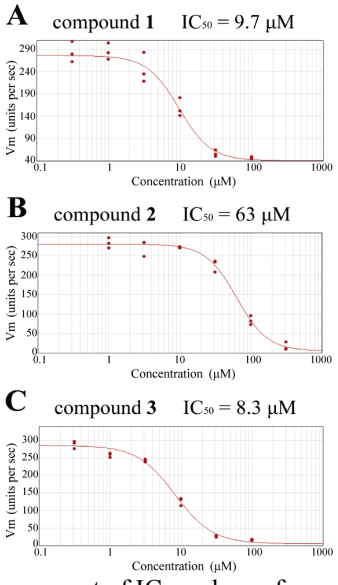

Figure 2: Measurement of IC_{50} values of compounds **1**-**3** using a FRET-based assay. V_m was measured in triplicate at each concentration for the respective compounds.

In protein crystallization, we used truncated PA_N ($PA_N^{\Delta loop}$) and obtained the co-crystal structure with one

of the inhibitors, compound **1**, in the $P4_12_12$ space group with one protein molecule in an asymmetric unit. It was shown in the crystal structure that three molecules of the inhibitor were bound to different positions in the active site (Figs. 3A, 3B).

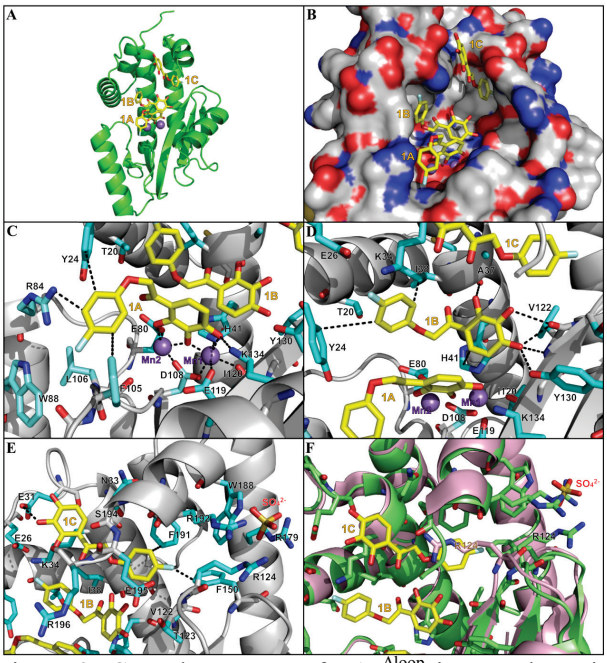

Figure 3: Crystal structure of $PA_N^{\Delta loop}$ in complex with compound **1**. (A) Overall structure of the complex. Protein backbone is depicted in cartoon (green), two manganese ions are in spheres (magenta), and three molecules of compound **1** are in the ball-and-stick model colored yellow (carbon), red (oxygen), and palecyan (fluorine). Three inhibitory molecules are labeled **1A**, **1B**, and **1C**. (B) Surface representation of the protein colored gray (carbon), red (oxygen), and blue (nitrogen). (C-E) Magnified images of the complex, in which the interactions of the protein with **1A** (C), **1B** (D), and **1C** (E) are depicted. The residues of the protein near the inhibitory molecules are represented in the ball-and-stick model colored cyan (carbon), red (oxygen), and blue (nitrogen) with the labels of their residue names, while other residues are shown in cartoon (gray). Interactions among the protein, metal ions, and compound **1** are depicted by black dotted lines. (F) Conformational change of R124 induced by the binding of compound **1**. The complex structure in this work (palegreen) is superimposed on chain A of 4AWG (PDB code, lightpink) for comparison. Only R124 is represented in the ball-and-stick model for 4AWG. It should be noted that the side chain of R124 is oriented in almost the opposite direction.

Molecule **1A** was coordinated to two manganese ions in the active center by its trihydroxyphenyl group, and *p*-fluorophenyl group of **1A** was extended toward the pocket made by Arg84, Trp88, Phe105, and Leu106 (Fig. 3C). The trihydroxyphenyl group of molecule **1B** made a π-π interaction with His41 and formed several hydrogen bonds with the target protein. The *p*-fluorophenyl group of **1B** was bound to the pocket formed by Thr20, Tyr24, Glu26, Lys34, and Ile38 (Fig. 3D). Compared with these two molecules, molecule **1C** had a unique binding mode, in which its *p*-fluorophenyl group was deeply inserted into the highly hydrophobic pocket (Fig. 3E). This pocket was comprised of Val122, Arg124, Phe150, Trp188, Phe191, Arg192, and Glu195 and was formed mainly due to the drastic conformational change of Arg124 as depicted in Fig. 4F. Originally, this arginine residue buried the pocket, making the protein surface positively charged (A representative structure is shown in lightpink in Fig. 3F.), and was sometimes utilized for polar interaction with some inhibitory compounds. However, in the case of molecule **1C**, the side chain of the arginine was oriented in almost the opposite direction and interacted with a sulfate ion (structure shown in palegreen in Fig. 3F), which allowed the compound to be fit for the hydrophobic pocket. This conformational change of Arg124 has not been observed in any previously reported crystal structures of PA_N. Some of those crystal structures were obtained under the crystallization conditions that include ammonium sulfate. Hence, the presence of ammonium sulfate had little influence on the conformational change of R124, which suggests that not sulfate ion but inhibitor molecule is an essential factor induce the conformational change. The three hydroxy groups and a carbonyl group at the opposite side of **1C** seem not to strongly interact with the residues of PA_N, while one hydrogen bond is observed between the 3-hydroxy group of **1C** and the side chain of E31 at a distance of 3.2 Å. Possibly, these polar moieties contribute to the binding affinity by covering the hydrophobic part of the compound and the protein, thereby increasing the polar surface area of the complex.

The binding site for molecule **1C** was not observed in the previous crystallographic studies. Hence, the stability of inhibitor binding was examined by performing 100-ns MD simulation. During the MD simulation, the three inhibitor molecules fluctuated at the respective binding sites at different amplitudes, while all of the molecules maintained interactions with the protein. Molecular mechanics/generalized Born surface area (MM/GBSA) analysis suggested that the molecule **1C** has a higher affinity than the others. Structural information obtained in this study will provide a hint for designing and developing novel potent agents against influenza viruses.

References

[1] S. Fudo, N. Yamamoto, M. Nukaga, T. Odagiri, M. Tashiro, S. Neya, T. Hoshino : Structural and computational study on inhibitory compounds for endonuclease activity of influenza virus polymerase, *Bioorganic & Medicinal Chemistry*, in press (2015).
[2] PDB code : 4YYL, 4ZHZ, 4ZI0, 4ZQQ

* hoshino@chiba-u.jp